

Generalized parton distributions: recent results^{*}

M. Diehl

Deutsches Elektronen-Synchrotron DESY, 22603 Hamburg, Germany

Abstract

I review progress on selected issues connected with generalized parton distributions. Topics range from the description of hard exclusive reactions to the spatial distribution of quarks in the nucleon and the contribution of their orbital angular momentum to the nucleon spin.

1 Introduction

An outstanding task in QCD is to understand hadron structure at the level of quarks and gluons. A wealth of information about this structure is contained in generalized parton distributions (GPDs). They are related both to the conventional parton densities and to elastic form factors—quantities which have played a crucial role in the understanding of strong interactions, and which at first sight are of very different nature. Recent reviews on GPDs can be found in [1, 2].

GPDs are defined through matrix elements $\langle p' | \mathcal{O} | p \rangle$ between hadron states $|p'\rangle$ and $|p\rangle$, with non-local operators \mathcal{O} constructed from quark and gluon fields. As sketched in Fig. 1a, GPDs depend on several kinematical variables, namely on the longitudinal momentum fractions $x + \xi$ and $x - \xi$ of the partons and on the invariant momentum transfer $t = (p - p')^2$. For unpolarized quarks there are two distributions $H^q(x, \xi, t)$ and $E^q(x, \xi, t)$. The former is diagonal in the proton helicity, whereas the latter describes proton helicity flip. For $p = p'$ and equal proton helicities one recovers the diagonal matrix element parameterized by usual quark and antiquark densities, so that $H^q(x, 0, 0) = q(x)$ and $H^q(-x, 0, 0) = -\bar{q}(x)$ for $x > 0$. Taking Mellin moments of in x , one obtains matrix elements of *local* operators, which are parameterized by form factors. In particular, the lowest moments give the well-known Dirac and Pauli form factors:

$$\sum_q e_q \int dx H^q(x, \xi, t) = F_1(t), \quad \sum_q e_q \int dx E^q(x, \xi, t) = F_2(t), \quad (1)$$

where e_q denotes the fractional quark charge. The ξ independence of the integrals is a consequence of Lorentz invariance. Of great interest is the next highest moment

$$\int dx x [H^q(x, \xi, t) + E^q(x, \xi, t)] = 2J^q(t), \quad (2)$$

because $J^q(0)$ gives the total angular momentum carried by quarks and antiquarks of a given flavor, including both their helicity and their *orbital* angular momentum. Belonging to local operators, the Mellin moments of GPDs are well suited for evaluation in lattice QCD (see below).

^{*}Talk presented at the Particles and Nuclei International Conference (PANIC 05), Santa Fe, NM, USA, 24–28 Oct. 2005. To appear in the Proceedings.

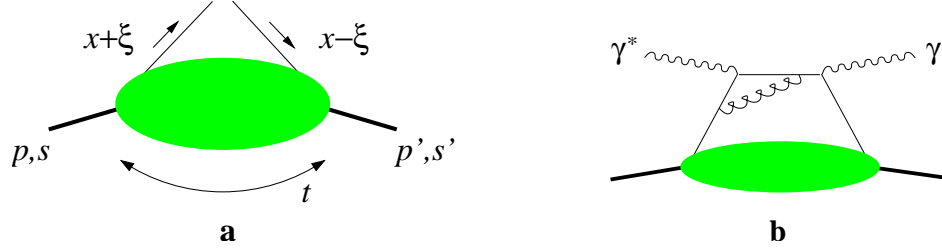


Figure 1: **a:** Variables in a GPD. The momentum fractions x and ξ refer to the average hadron momentum $\frac{1}{2}(p + p')$. **b:** A graph for the amplitude of deeply virtual Compton scattering (DVCS).

Factorization theorems state that GPDs appear in the scattering amplitudes of suitable hard exclusive processes. Figure 1b shows an example graph for deeply virtual Compton scattering, $\gamma^* p \rightarrow \gamma p$, where a hard scale is provided by the initial photon virtuality. A large number of reaction channels can be accessed in hard exclusive meson production, such as $\gamma^* p \rightarrow \rho p$ or $\gamma p \rightarrow J/\Psi p$, where in addition to quark or gluon GPDs the quark-antiquark distribution amplitudes of the meson appear as non-perturbative input (see Fig. 2). The longitudinal momentum transfer ξ is fixed by the process kinematics (for DVCS and light meson production one simply has $\xi = x_B/(2 - x_B)$ in terms of the usual Bjorken variable). In contrast, x is a loop variable, and ξ only gives the *typical* size of x in the convolution of the GPD with the hard-scattering amplitude. The hard-scattering subprocesses for Compton scattering, electroproduction of light mesons, and photoproduction of heavy quarkonium are fully calculated at next-to-leading order (NLO) in α_s , and partial results for DVCS at NNLO have just appeared [3]. Whereas α_s corrections are generally found to be moderate for Compton scattering, they can be substantial for meson production [4], and more detailed studies will be needed to gain quantitative theoretical control over these channels.

In addition to the variables already discussed, GPDs depend on the scale at which the partons are resolved, given by the hard scale in the physical process. The evolution equations for GPDs interpolate between those for ordinary parton densities and those for meson distribution amplitudes. The evolution kernels are known to NLO in α_s , but it is only recently and only to LO accuracy that one has an explicit solution of the evolution equations [5, 6]. Generalizing the well-known Mellin transform technique employed for the ordinary parton densities, this solution should be useful both for efficient numerical implementation and for analytic considerations, for instance in the limit of small x .

A typical strategy for modeling GPDs is to take an ordinary parton density as input and to generate a ξ dependence consistent with Lorentz invariance relations, which state that Mellin moments in x

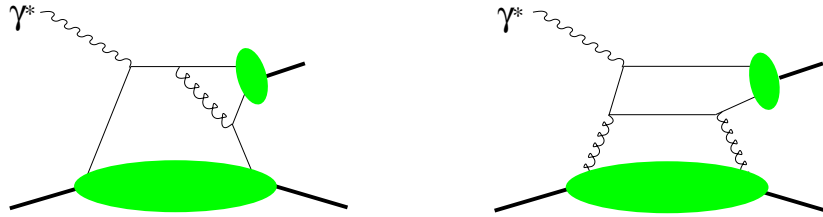


Figure 2: Example graphs for exclusive meson production. The large blobs represent GPDs and the small ones the distribution amplitudes of the produced meson.

of GPDs must be polynomials in ξ of a specified degree. Different ansätze are used to this end, the most common ones being based on so-called double distributions [7] or on the evolution of GPDs at small x and ξ [8]. Different strategies based on moments have recently been proposed in [6] and in [9]. With the Compton amplitude calculated at LO in α_s , the model in [9] provides a good description of the data [10, 11] for DVCS at small x_B . The t dependence of GPDs will be discussed below.

2 Vector meson production

An important feature of exclusive vector meson production is that quark and gluon distributions appear at the same order in α_s , whereas in DVCS (just as in inclusive deep inelastic scattering) the gluon contribution is suppressed by α_s relative to quarks. Schematically, one has

$$\mathcal{A}_{\rho^0} \propto \frac{1}{\sqrt{2}} \left[\frac{2}{3}(u + \bar{u}) + \frac{1}{3}(d + \bar{d}) + \frac{3}{4}g \right], \quad \mathcal{A}_{\phi} \propto \frac{1}{3}(s + \bar{s}) + \frac{1}{4}g, \quad (3)$$

where $u + \bar{u}$, $d + \bar{d}$, $s + \bar{s}$, and g represent the convolutions of the relevant GPDs with the hard-scattering kernels (which are identical for quarks and gluons at LO). Taking the ordinary parton densities as a rough guide for the relative size of terms in (3), one expects that, even in kinematics of the fixed-target experiments at HERMES and Jefferson Lab, gluons provide a substantial contribution to the ρ^0 production amplitude. This expectation is supported by preliminary HERMES data for the ratio of ϕ and ρ^0 production cross sections [12]. The same conclusion has been reached in an explicit calculation with GPD models based on double distributions [13]. In the same analysis, substantial changes in the calculated cross sections at $Q^2 \sim 4 \text{ GeV}^2$ and $x_B \sim 0.1$ were found when taking different parameterizations of the gluon density as input to the GPD model. This reflects on one hand the present uncertainty in our knowledge even of the ordinary gluon distribution, and on the other hand the sensitivity of meson production to the generalized gluon distribution. Very similar findings were made in the study [14] of exclusive J/Ψ production at collider energies: the high-precision data [15] clearly disfavor a number of parameterizations of the gluon density in conjunction with the Shuvaev model [8] for the ξ dependence of the gluon GPD.

It has long been known that in exclusive meson production the leading-twist approximation, which gives the leading term in a $1/Q$ expansion, overshoots the data by factors of several for photon virtualities Q^2 below 5 GeV^2 . Closer analysis reveals that important corrections to this approximation can be ascribed to the effect on the hard-scattering amplitude of the intrinsic transverse momentum of quarks in the produced meson. A recent analysis [16] modeling this effect finds good agreement with ρ^0 and ϕ production data at high energies from H1 and ZEUS.

3 Impact parameter distributions

An important feature of GPDs is that they contain information about the spatial distribution of quarks and gluons in the nucleon. This becomes explicit in the impact parameter representation [17] (for different approaches see [18] and [19]). To introduce this representation, let us form wave packets

$$|p^+, \mathbf{b}\rangle = \int \frac{d^2p}{(2\pi)^2} e^{-i\mathbf{b}\mathbf{p}} |p^+, \mathbf{p}\rangle \quad (4)$$

from momentum eigenstates $|p^+, \mathbf{p}\rangle$, where the plus-momentum $p^+ = (p^0 + p^3)/\sqrt{2}$ simply becomes the longitudinal momentum (up to a factor $\sqrt{2}$) in a frame where the proton moves fast. The conjugate variable to the transverse momentum $\mathbf{p} = (p^1, p^2)$ is called impact parameter \mathbf{b} and gives the position of the wave packet in the transverse plane. Indeed, $|p^+, \mathbf{b}\rangle$ is an eigenstate of a suitably defined

transverse position operator, i.e., a relativistic particle can be localized *exactly* in two dimensions (without the ambiguities at the order of a Compton wavelength occurring when one attempts to localize a particle in all three dimensions). A more detailed analysis shows that \mathbf{b} is the “center of momentum” of the partons in the proton, given by a weighted average $\mathbf{b} = \sum_i p_i^+ \mathbf{b}_i / \sum_i p_i^+$ in terms of their plus-momenta and transverse positions. The center of momentum is related by Noether’s theorem to a class of Lorentz transformations called “transverse boosts”, in analogy to the relation between the center of mass and Galilean transformations in nonrelativistic mechanics.

Forming matrix elements from impact parameter states (4) and the operators defining generalized parton distributions in momentum space, one obtains Fourier transforms of these distributions. For $\xi = 0$ one finds that

$$q(x, b^2) = \int \frac{d^2 \Delta}{(2\pi)^2} e^{-i\mathbf{b}\Delta} H^q(x, 0, -\Delta^2) \quad (5)$$

is the density of quarks with longitudinal momentum fraction x and transverse distance \mathbf{b} from the center of momentum of the proton. Integrating $q(x, b^2)$ over \mathbf{b} one recovers the usual quark distribution. For $\xi \neq 0$ one no longer has a probability interpretation because the two momentum fractions in Fig. 1a are different, but \mathbf{b} still describes the distribution of the struck parton in the transverse plane. According to the discussion in the introduction, the combined ξ and t dependence of hard exclusive processes thus gives information about the impact parameter distribution of partons with longitudinal momentum fraction of order ξ . Precise measurements are in particular available for the t dependence of J/Ψ production [15], giving access to the spatial distribution of small- x gluons. H1 has published a first result for the t dependence of DVCS [11], which at the small x_B of the measurement is sensitive to a combination of sea quark and gluon distributions.

Like ordinary parton densities, the impact parameter distributions $q(x, b^2)$ and $g(x, b^2)$ for quarks and gluons depend on the resolution scale μ . Their scale evolution is local in \mathbf{b} and described by the usual DGLAP equations. As a consequence, the \mathbf{b} dependence of the distributions at given x also changes with μ . A useful quantity to characterize the \mathbf{b} distribution is the average squared impact parameter, defined as

$$\langle b^2 \rangle_x = \frac{\int d^2 b \, b^2 q(x, b^2)}{\int d^2 b \, q(x, b^2)} = 4 \frac{\partial}{\partial t} \log H^q(x, 0, t) \Big|_{t=0} \quad (6)$$

for quarks and in analogy for gluons. It is straightforward to obtain the evolution equations for $\langle b^2 \rangle_x$ from those for the impact parameter distributions [20].

When a quark takes most of the proton momentum, its impact parameter will tend to coincide with the center of momentum of the proton as a whole. For $x \rightarrow 1$ one therefore expects a narrow distribution in \mathbf{b} , or equivalently a flat t dependence of GPDs in momentum space. An estimate for the overall transverse size of the proton in that limit is given by the transverse distance $\mathbf{b}/(1-x)$ between the struck quark and the center of momentum of the *spectator* partons, as shown in Fig. 3. It seems plausible to assume that this distance remains finite due to confinement [21], so that the average squared impact parameter of partons should vanish like $\langle b^2 \rangle_x \sim (1-x)^2$ for $x \rightarrow 1$. In the opposite limit of small x , the phenomenology of high-energy hadronic reactions suggests a behavior like $x^{-(\alpha+\alpha't)} e^{tB}$ of momentum-space GPDs [1, 20]. According to (6) this translates into a logarithmic growth of the average impact parameter as x becomes small, $\langle b^2 \rangle_x \sim B + \alpha' \log(1/x)$.

Indirect information on impact parameter distributions can be obtained by using the sum rules (1) and the extensive and precise data on the nucleon form factors [20, 22]. For the Dirac form factor $F_1(t)$ this requires an ansatz for the functional dependence of $H^q(x, 0, t)$, which can be restricted to its valence part, since the electromagnetic current is only sensitive to the difference of quark and antiquark distributions. A crucial result of such studies is the rapid decrease of the average impact

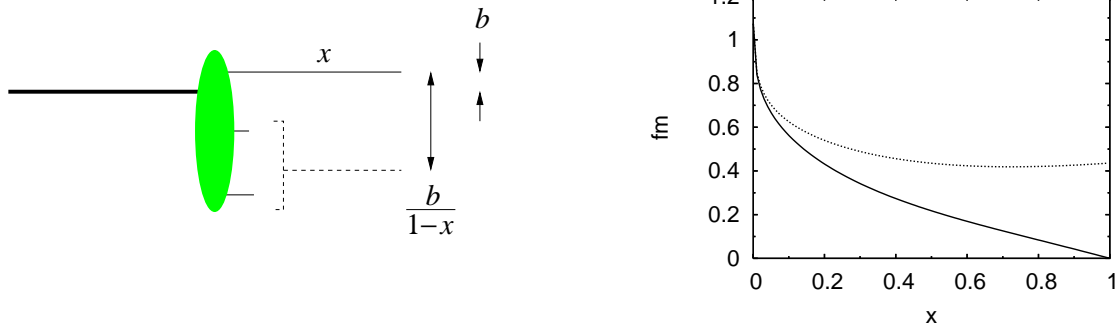


Figure 3: Left: Three-quark configuration with one fast quark in a proton. The thick line denotes the center of momentum of the proton and the dashed line the center of momentum of the two spectator quarks. Right: Average impact parameter $\sqrt{\langle b^2 \rangle_x}$ of the valence u quark distribution (lower curve) and the associated distance $(1-x)^{-1}\sqrt{\langle b^2 \rangle_x}$ between the struck parton and the center of momentum of the spectators (upper curve), as estimated in [20].

parameter with x over the entire x range, as illustrated for the distribution $u(x, b^2) - \bar{u}(x, b^2)$ in Fig. 3. In momentum space, this corresponds to a t dependence that becomes less steep with increasing x . This finding is confirmed by calculations in lattice QCD, where a clear decrease of the t slope is seen for moments $\int dx x^n H^q(x, 0, t)$ with increasing power n [23].

A strong correlation between the transverse distribution of partons and their momentum fraction is not only interesting from the perspective of hadron structure, but also has practical consequences for high-energy hadron-hadron collisions [24]. Consider the production of a high-mass system (e.g. a dijet or a heavy particle). For the inclusive production cross section, the distribution of the colliding partons in impact parameter is not important: only the parton distributions integrated over impact parameters are relevant according to standard hard-scattering factorization (see Fig. 4a). There can however be additional interactions in the same collision, especially at the high energies of the Tevatron or the LHC, as shown in Fig. 4b. Their effect cancels in sufficiently *inclusive* observables, but it does affect the event characteristics and can hence be quite relevant in practice. In this case, the impact parameter distribution of partons does matter: the production of a heavy system requires large momentum fractions for the colliding partons. A narrow impact parameter distribution for these partons forces the collision to be more central, which in turn increases the probability for multiple parton collisions in the event.

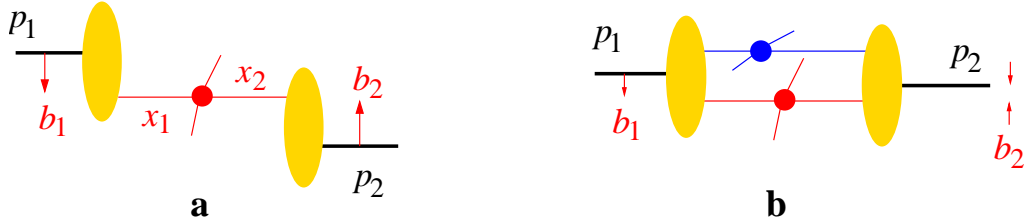


Figure 4: **a:** Graph with a single hard interaction in a hadron-hadron collision. The impact parameters b_1 and b_2 are integrated over independently. **b:** Graph with a primary and a secondary interaction.

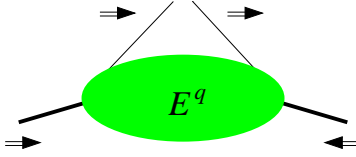


Figure 5: A transition where the proton helicity is flipped but the quark helicity conserved. The helicity mismatch is compensated by one unit of orbital angular momentum, so that angular momentum is conserved.

4 Spin and orbital angular momentum

The proton helicity-flip distributions E^q have a density interpretation at $\xi = 0$, similar to the distributions H^q discussed so far. To see this one changes basis from proton helicity states $|\uparrow\rangle, |\downarrow\rangle$ to states $|X\pm\rangle = (|\uparrow\rangle \pm |\downarrow\rangle)/\sqrt{2}$ polarized along the positive or negative x axis. In impact parameter space one then obtains the density

$$q_X(x, \mathbf{b}) = q(x, b^2) - \frac{b^y}{m} \frac{\partial}{\partial b^2} e^q(x, b^2) \quad (7)$$

of unpolarized quarks in a proton polarized along the positive x direction, where the Fourier transform

$$e^q(x, b^2) = \int \frac{d^2\Delta}{(2\pi)^2} e^{-i\mathbf{b}\Delta} E^q(x, 0, -\Delta^2) \quad (8)$$

is defined in analogy to (5) and m denotes the nucleon mass. The impact parameter distribution of quarks in a transversely polarized proton is thus shifted in the direction perpendicular to the polarization. This shift must be substantial at least for some x and \mathbf{b} : due to the sum rule (1) the average $\int dx \int d^2b e^q(x, b^2) = \kappa^q$ is given by the magnetic moments of proton and neutron as $\kappa^u \approx 1.67$ and $\kappa^d \approx -2.03$ and hence quite large. A connection has been proposed in [25] between the anisotropy (7) in the *spatial* distribution of quarks and the Sivers effect, which is an anisotropic *transverse momentum* distribution of quarks in a transversely polarized proton. The Sivers effect has indeed been observed experimentally [26]. Similar asymmetries can be discussed for the distribution of transversely polarized quarks in an unpolarized proton [27], and first results in lattice QCD indicate that the corresponding anisotropy of the impact parameter distribution is appreciable [28].

The interpretation of (7) as a density implies positivity conditions for $e^q(x, b^2)$ [29]. In momentum space one has a simple bound

$$|E^q(x, 0, 0)| \leq q(x) m \sqrt{\langle b^2 \rangle_x}, \quad (9)$$

with more stringent inequalities involving also quark helicity dependent distributions on the right-hand side. According to the behavior of $\langle b^2 \rangle_x$ discussed in the previous section, this restricts E^q quite severely at larger values of x . The distribution E^q involves one unit of orbital angular momentum since in the associated matrix elements the proton helicity is flipped but the quark helicity conserved (see Fig. 5). The bound (9) thus limits the amount of orbital angular momentum that can be carried by quarks [30], and is especially strong at large x .

Further information on the helicity-flip distribution can be obtained from the sum rule for the Pauli form factor in (1). For this one needs an ansatz for the valence part of $E^q(x, 0, t)$, which can be made in analogy to the case of $H^q(x, 0, t)$ and the Dirac form factor [20, 22]. The corresponding fits are less well constrained, because in contrast to H^q the forward limit $E^q(x, 0, 0)$ is not known and needs to be parameterized in addition to t dependence of E^q . It turns out that the positivity bound

(9) and its stronger versions provide valuable restrictions of the allowed parameter space. One can use these restrictions and estimate the total angular momentum J_v^q carried by valence quarks, taking the analog of Ji's sum rule (2) for the difference of quark and antiquark contributions. The result obtained in [20, 31] is $2J_v^u = 0.39 \div 0.46$ and $2J_v^d = -0.04 \div 0.04$ at scale $\mu = 2$ GeV. Subtracting the quark helicity parts, one gets rather large numbers $2L_v^u = -(0.47 \div 0.54)$ and $2L_v^d = 0.30 \div 0.38$ for the orbital angular momentum carried by u and d valence quarks. The corresponding estimate for the isovector combination $2(L_v^u - L_v^d) = -(0.77 \div 0.92)$ is large, whereas the isoscalar combination $2(L_v^u + L_v^d) = -(0.11 \div 0.22)$ is uncertain and quite small. Lattice calculations by the QCDSF Collaboration obtain $2(L^u - L^d) = 0.90 \pm 0.12$ and $L^u + L^d$ compatible with zero within errors [32]. Given the very different sources of systematic errors in the lattice evaluation and the estimate from [20, 31], the agreement between the two is encouraging, especially for the isovector combination, where sea quark contributions should be small.

The angular momentum carried by sea quarks is hardly known. It cannot be inferred from electromagnetic form factors, and in lattice QCD it requires calculation of so-called “disconnected” graphs, which are affected by large statistical errors. Information on sea quarks can however be obtained from hard exclusive processes, especially from DVCS, where the control of theory is highest and a large number of spin asymmetries can be evaluated in the leading-twist approximation. HERMES has presented preliminary results for the spin asymmetry in DVCS on a transversely polarized proton [33]. Their comparison with a calculation [34] using J^q as input parameter in the ansatz for E^q shows that this asymmetry is indeed sensitive to J^u in the kinematics of the experiment (recall that in Compton scattering on the proton u and d quark distributions have relative weight 4 : 1 due to the squared quark charges). A measurement of DVCS on the neutron at Jefferson Lab Hall A [35] is currently being analyzed and should provide information about J^d . A number of ongoing measurements at Jefferson Lab and DESY can provide information on the unpolarized distributions H^q and \bar{H}^q . Future experimental prospects for this field are a proposed run of COMPASS at CERN with a detector for recoiling protons [36], the planned upgrade of Jefferson Lab to 12 GeV, and eventually an electron-proton collider eRHIC/EIC.

5 Conclusions

In this talk I have reviewed progress in selected areas connected with generalized parton distributions. There are many interesting aspects discussed in the recent literature which I could not cover for reasons of time. Among these are studies of GPDs in dynamical models, GPDs of nuclei, production of exotic mesons, GPDs for hadron-photon and baryon-meson transitions, hard exclusive processes at large s and t , and possibilities to study GPDs in neutrino-nucleon scattering with future high-intensity neutrino beams.

To summarize, there has been important technical progress in the description of hard exclusive processes, with full NLO results in α_s available for most relevant channels, partial NNLO results for Compton scattering, and a better understanding of the scale evolution of GPDs. These advances remain to be fully implemented in the analysis of data, but existing studies have in particular shown the high sensitivity of vector meson production to the generalized gluon distribution, even at the moderate x accessible in fixed-target experiments.

Through the impact parameter representation, GPDs provide information on the spatial distribution of partons in a hadron, and a number of studies have turned this concept into quantitative information. Phenomenological analysis of elastic form factors, as well as results from lattice QCD show that the average impact parameter of valence quarks strongly decreases with their momentum fraction in the proton. The proton helicity-flip distribution E^q has connections with two crucial aspects of spin physics: transverse polarization effects and the orbital angular momentum L^q carried

by quarks in the nucleon. First steps have been taken towards a quantitative understanding of L^q . The present picture—suggested both by lattice results and model-dependent analysis of experimental data—is that for individual quark flavors L^q may be substantial, but that when summed over flavors the orbital angular momentum carried by *valence* quarks contributes little to the nucleon spin. The proton spin puzzle thus remains a puzzle.

Acknowledgments

I thank the Conference Organizers for the kind invitation to attend this very fruitful meeting. This work is supported by the Helmholtz Association, contract number VH-NG-004.

References

- [1] K. Goeke et al., Prog. Part. Nucl. Phys. **47**, 401 (2001) [hep-ph/0106012].
- [2] M. Diehl, Phys. Rept. **388**, 41 (2003) [hep-ph/0307382];
A. V. Belitsky and A. V. Radyushkin, Phys. Rept. **418**, 1 (2005) [hep-ph/0504030].
- [3] D. Müller, hep-ph/0510109.
- [4] A. V. Belitsky and D. Müller, Phys. Lett. B **513**, 349 (2001) [hep-ph/0105046];
D. Yu. Ivanov et al., Eur. Phys. J. C **34**, 297 (2004) [hep-ph/0401131];
D. Yu. Ivanov, L. Szymanowski and G. Krasnikov, JETP Lett. **80**, 226 (2004) [hep-ph/0407207].
- [5] M. Kirch, A. Manashov and A. Schäfer, hep-ph/0509330;
A. Manashov, M. Kirch and A. Schäfer, Phys. Rev. Lett. **95**, 012002 (2005) [hep-ph/0503109].
- [6] D. Müller and A. Schäfer, hep-ph/0509204.
- [7] I. V. Musatov and A. V. Radyushkin, Phys. Rev. D **61**, 074027 (2000) [hep-ph/9905376].
- [8] A. G. Shuvaev et al., Phys. Rev. D **60**, 014015 (1999) [hep-ph/9902410].
- [9] V. Guzey and M. V. Polyakov, hep-ph/0507183.
- [10] S. Chekanov et al. [ZEUS Collaboration], Phys. Lett. B **573**, 46 (2003) [hep-ex/0305028].
- [11] A. Aktas et al. [H1 Collaboration], Eur. Phys. J. C **44**, 1 (2005) [hep-ex/0505061].
- [12] M. Diehl and A. V. Vinnikov, Phys. Lett. B **609**, 286 (2005) [hep-ph/0412162].
- [13] M. Diehl, W. Kugler, A. Schäfer and C. Weiss, Phys. Rev. D **72**, 034034 (2005) [hep-ph/0506171].
- [14] T. Teubner, Proceedings of DIS 2005, AIP Conference Proceedings **792**, 416 (2005).
- [15] ZEUS Collaboration, Nucl. Phys. B **695**, 3 (2004) [hep-ex/0404008];
A. Aktas et al. [H1 Collaboration], hep-ex/0510016.
- [16] S. V. Goloskokov and P. Kroll, Eur. Phys. J. C **42**, 281 (2005) [hep-ph/0501242].
- [17] M. Burkardt, Int. J. Mod. Phys. A **18**, 173 (2003) [hep-ph/0207047];
M. Diehl, Eur. Phys. J. C **25**, 223 (2002), Erratum ibid. C **31**, 277 (2003) [hep-ph/0205208].
- [18] J. P. Ralston and B. Pire, Phys. Rev. D **66**, 111501 (2002) [hep-ph/0110075].

- [19] A. V. Belitsky, X. D. Ji and F. Yuan, Phys. Rev. D **69**, 074014 (2004) [hep-ph/0307383].
- [20] M. Diehl, T. Feldmann, R. Jakob and P. Kroll, Eur. Phys. J. C **39**, 1 (2005) [hep-ph/0408173].
- [21] M. Burkardt, Phys. Lett. B **595**, 245 (2004) [hep-ph/0401159].
- [22] M. Guidal et al., Phys. Rev. D **72**, 054013 (2005).
- [23] J. W. Negele et al., Nucl. Phys. Proc. Suppl. **128**, 170 (2004) [hep-lat/0404005];
M. Göckeler et al. [QCDSF Collaboration], Nucl. Phys. A **755**, 537 (2005) [hep-lat/0501029].
- [24] L. Frankfurt, M. Strikman and C. Weiss, Phys. Rev. D **69**, 114010 (2004) [hep-ph/0311231];
M. Strikman and C. Weiss, these proceedings.
- [25] M. Burkardt and D. S. Hwang, Phys. Rev. D **69**, 074032 (2004) [hep-ph/0309072].
- [26] A. Airapetian et al. [HERMES Collaboration], Phys. Rev. Lett. **94**, 012002 (2005) [hep-ex/0408013];
B. Zihlmann, these proceedings.
- [27] M. Diehl and Ph. Hägler, Eur. Phys. J. C **44**, 87 (2005) [hep-ph/0504175];
M. Burkardt, Phys. Rev. D **72**, 094020 (2005) [hep-ph/0505189].
- [28] M. Diehl et al. [QCDSF Collaboration], hep-ph/0511032.
- [29] M. Burkardt, Phys. Lett. B **582**, 151 (2004) [hep-ph/0309116].
- [30] M. Burkardt and G. Schnell, hep-ph/0510249.
- [31] M. Diehl, hep-ph/0510221.
- [32] G. Schierholz, Proceedings of DIS 2005, AIP Conference Proceedings **792**, 929 (2005).
- [33] Z. Ye, hep-ex/0512010.
- [34] F. Ellinghaus, W. D. Nowak, A. V. Vinnikov and Z. Ye, hep-ph/0506264.
- [35] P. Bertin et al., Jefferson Lab Experiment E03-106.
- [36] N. d'Hose et al., hep-ex/0212047.